

Seismicity relocation and fault structure near the Leech River Fault Zone, southern Vancouver Island

Ge Li^{1*}, Yajing Liu¹, Christine Regalla² and Kristin Morell³

1. Department of Earth and Planetary Sciences, McGill University, Montreal, H3A 0E8, Canada

2. Department of Earth and Environment, Boston University, Boston, 02215, USA

3. School of Earth and Ocean Sciences, University of Victoria, British Columbia, V8P 5C2, Canada

*Corresponding Author: Phone: 514-839-9916, Email: ge.li2@mail.mcgill.ca

Abstract

By analyzing high-precision microseismicity relocation, we provide the first evidence to delineate potentially crustal seismogenic structures and their seismic behaviors associated with the Leech River Fault Zone (LRFZ) on southern Vancouver Island. Our data reveal a zone of seismicity delineating a major subsurface structure striking along the eastern 30 km of the terrestrial LRF that extends eastward for 20 km beneath the Juan de Fuca Strait. As suggested by clustering, the complex spatial distribution of crustal seismicity delineates a wide steeply NNE-dipping structure in the western half of the study area that bifurcates into two fault zones farther to the east. Our results also reveal several secondary, linear structures with right-lateral strike-slip faulting mode developed within the major structure NNE-dipping structure. This network of fractures is interpreted to act as a single diffuse fault zone, which may be related to recently documented Quaternary surface scarps along the LRF.

1. Introduction

Vancouver Island is located along the northern Cascadia subduction zone in southwest British Columbia, and is considered one of the most seismically active zones in Canada [Kovacs and Sweeting, 2004]. Despite evidence for abundant crustal seismicity on this island, it remains difficult to correlate microseismicity to mapped surficial fault traces [Rogers, 1994; Mosher et al., 2000; Cassidy et al., 2000], and the geometry and kinematics of potentially seismogenic faults are usually not well known. Here, we investigate seismicity near the Leech River Fault Zone (LRFZ), one of the most prominent fault systems on the southern Vancouver Island, which extends for ~60 km along strike (Figure 1). The fault has been imaged, based on the Lithoprobe profile, as a NNE ~45° dipping fault extending to ~10km [Clowes et al. 1987] and classically interpreted as inactive since the Eocene [MacLeod et al., 1977; Cassidy et al., 2000; Mosher et al., 2000]. However, recent field and LiDAR evidence reveals sub-parallel, steeply dipping topographic features that suggest late Quaternary activity on this fault [Morell et al, 2017]. To investigate the geometry and kinematics potential seismogenic structures associated with this fault, we use a double-difference earthquake location algorithm (HypoDD) to relocate earthquakes near the LRFZ and further analyze relocated earthquakes using several clustering methods. Based on our results, we interpret the source properties of these crustal earthquakes in the context of regional geology.

2. Method & Data

The relocation method used here is HypoDD double-difference program [Waldhauser and Ellsworth 2000], which can provide highly precise relative hypocenters by minimizing travel-time double-differences. We relocated 1253 earthquakes with local magnitudes (M_L) ranging from 0.1 to 4.9, reported by the CNSN

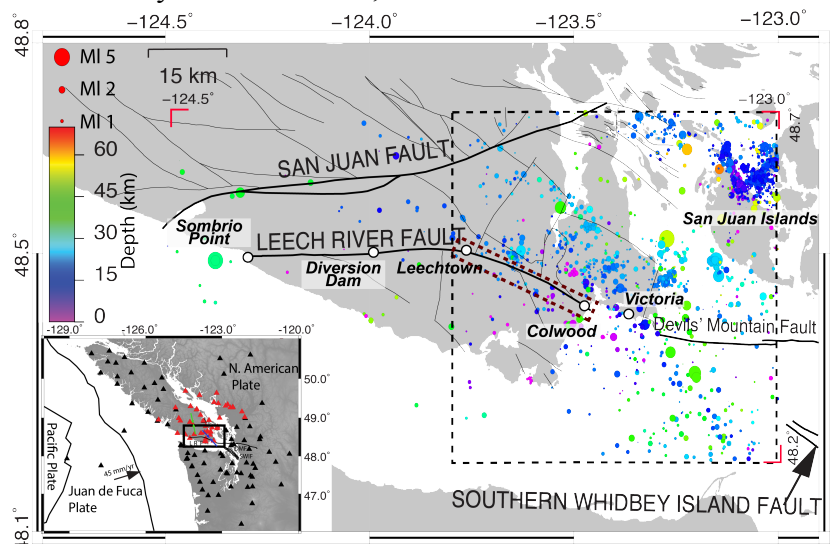


Figure 1. Tectonic setting of the study area showing catalog earthquakes locations and mapped faults in British Columbia. Black dashed-line box represents our study area, as in Figure 2. Brown dashed-line box represents the study region in Morell et al. [2017]. Red corners bracket the area for earthquakes analysed. Inset: Triangles denote the location of stations used for catalog phase arrivals (Red: phase arrivals from manual picks and waveform cross-correlation). Two maximum horizontal compression orientations inverted from earthquake focal mechanisms are also shown, S_{Hmax1} in green and S_{Hmax2} in blue [Balfour et al., 2011].

catalog between January 1992 and March 2015 within our study area near the LRFZ (Figure 1). A 1-D velocity model [Ramachandran et. al. 2006] is used in this paper: $(z, V_p) = (0, 4.5; 4.0, 5.5; 10.0, 6.75; 35.0, 6.9; 40.0, 7.75; 45.0, 8.0)$, where z is the depth of the top of the layer in km and V_p is P-wave velocity in km/s. V_s is set to be $V_p/\sqrt{3}$.

We construct the differential travel time datasets from the following two separate sources: 1) P/S arrivals provided by the CNSN catalog (Figure 1); 2) P/S differential times determined from waveform cross-correlation. The full dataset used for relocation consists of 91,505 differential times for P arrivals and 82,752 for S arrivals. Relocation uncertainties for the entire catalog were estimated statistically using a bootstrap method [Waldhauser and Ellsworth, 2000]. Resulting average bootstrapping errors for this relocation procedure are 142.7 m, 133.3 m and 286.8 m respectively in east, north and vertical directions.

3. Relocation Results

We focus our analysis on seismicity in the vicinity of the LRF (Figure 2). In cross-sectional view, earthquakes in this area can be divided into two groups: upper continental seismicity (depth < 30 km) and underlying slab seismicity, separated by a ~10 km thick gap zone (Figure 3), which coincides with a highly reflective zone bounded by what are generally termed as E-reflectors [Clowes et. al., 1987]. Events with depths less than 30 km are analyzed to investigate crustal faulting structures. Since most crustal earthquakes deviate from the LRF as imaged in the LITHOPROBE, it may suggest that the original lithological contact are not responsible for crustal seismic activities here.

Crustal earthquakes are projected onto five profiles (P1 to P5) perpendicular to the LRF surface trace between Leechtown and Colwood and its offshore extension (Figure 2a&b). To describe the spatial pattern of seismicity within each profile, two quantitative coefficients are used: linearity L and correlation coefficient C . They are defined as:

$$L = 1 - \frac{\lambda_2}{\lambda_1} \quad (\lambda_1 \text{ and } \lambda_2 \text{ are the maximum and minimum eigenvalues of the covariance matrix of the seismic spatial locations in } (X, Z) \text{ coordinates});$$

C : correlation coefficient value that measures the linear relationship between X and Z . A potential fault structure highlighted by seismicity is expected to have a large L value. As shown in Figure 2b, both the L and C values decrease eastward from P1 to P5, with a C value of nearly 0 at P5.

In general, higher L and C values at P1 to P3 suggest that seismicity delineates a continuous NNE dipping structure from P1 to P3. From P4 to P5, it becomes impossible to fit the data into a single dipping structure due to a near-zero C value. On each profile, seismicity appears to be a network of linear structures embedded in a broad, diffusive zone. In order to distinguish

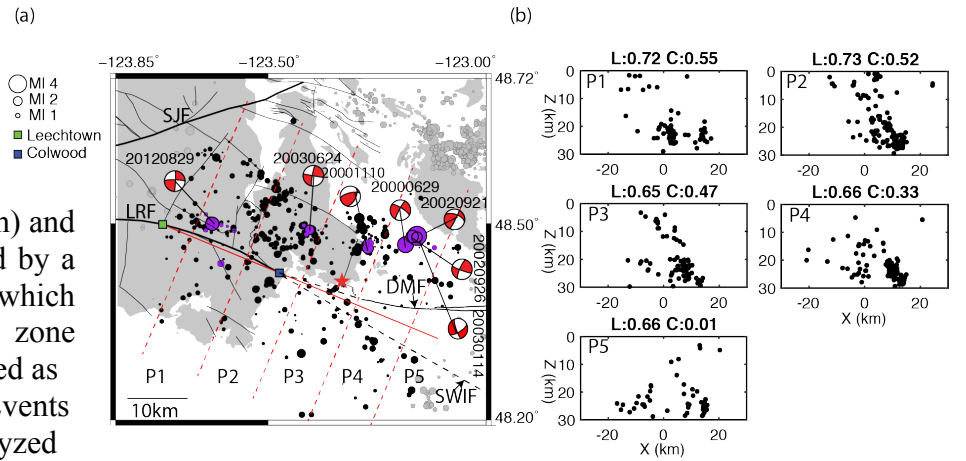


Figure 2. a) Relocated crustal earthquakes. Black and purple (repeating events, some with focal mechanism solutions) dots represent earthquakes analyzed in b). Grey dots represent background seismicity. Red dashed lines P1-P5 represent cross sections shown in following sections. Red solid line connecting the Leechtown and Colwood is the 'zero x-position line' of P1 to P5. The black dashed line represents the proposed offshore extension of the LRF to the strike of the SWIF and DMF. b) Cross-sectional view of crustal earthquakes along profiles P1-P5. Events within 5 km normal distance from each profile are plotted. L : linearity value; C : Correlation coefficient.

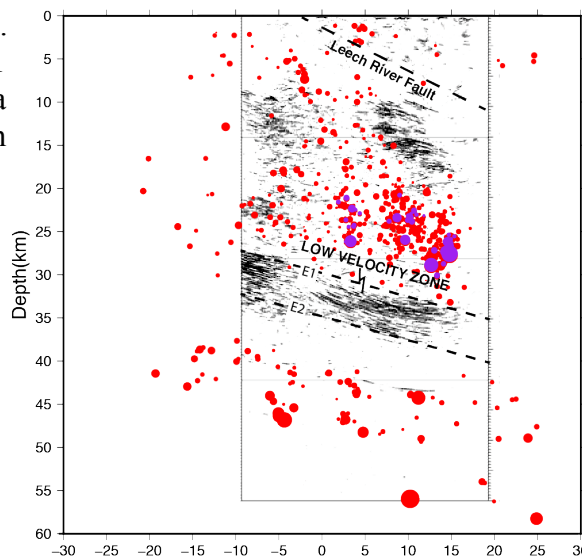


Figure 3. Relocated earthquakes projected along profile P1 with background image as seismic reflection results from Lithoprobe Line 02, normal to LRF. Thick dashed line above 10 km denotes Lithoprobe inferred LRF as the geological terrane boundary. E1 and E2 denote the top and bottom reflectors of inferred high reflection zone (also termed low velocity zone), respectively.

active structures from the background seismicity and reveal the spatial variation along the LRF, we apply a clustering analysis to the relocated earthquakes as described in following section.

4. Cluster Analysis and Results

Two clustering methods are applied to identify seismic clusters from relocated earthquakes: 1) the Gaussian Mixture Model (GMM) method, which quantifies high statistical significance in spatial locations, and 2) waveform cross-correlation in search of repeating events (RE) indicative of seismic energy radiation from common sources, complemented by focal mechanism solutions.

The GMM method is a statistical analysis method that divides a spatial distribution of points into any given number (k) of groups by maximizing the distribution likelihood function representing a mixture of several multivariate Gaussian Models [McLachlan and Peel, 2000]. We utilize a multi-level strategy to determine seismic clusters using the GMM method. First, we divide each profile of seismicity into k GMM groups, each group consisting of a minimum of 10 events and with a linearity coefficient greater than L_0 . Second, we vary k from 2 to 9 and repeat step 1. Finally, we retain stable clusters for subsequent interpretations. Several cutoff values are used in the above analysis. Using these criteria, we then define a stable cluster as any GMM group that survives at least 4 clustering scenarios, which is half of a total of 8 runs for $k = 2$ to 9. In order to test the influence of L_0 on cluster identification, we varied the linearity cut-off value L_0 from 0.5 to 0.9. We note that different choices of L_0 may result in slightly different stable clusters, e.g. a stable structure that survives 4 runs with a L_0 of 0.7 may only survive 3 runs (insufficient stability) when L_0 is increased to 0.8. In practice, however, the influence of L_0 on the determination of stable structures can be negligible.

To further test the robustness of the GMM determined structures, we performed repeating earthquake analysis to search for event pairs with highly similar waveforms which characterize repeated rupture of the same fault patch [Gardonio et al., 2015]. Repeating events (RE) pairs are defined as those closely spaced (<5km) earthquakes with waveform cross-correlation coefficient greater than 0.9 detected at ≥ 4 stations. RE pairs can then be grouped spatially into RE groups linked by common events [Nadeau et al., 1995]. This procedure results in 45 RE pairs, which constitute 10 RE groups with the largest group containing 10 events. Based on P polarities using the HASH package [Hardebeck and Shearer, 2003], we also calculated focal mechanism solutions for REs with magnitudes > 2.0 to provide insights in the faulting behavior of potential structures.

Figure 4 shows the final clustering results determined by these two methods. 7 clusters, indicative of seismic structures, are identified, including two vertical structures located in profile P1 (Cluster 1 and 2), two NNE dipping structures in P3 (Cluster 3 and 4), a NNE dipping structure in P4 (Cluster 5), a vertical structure, Cluster 7, and a moderately SW dipping ($\sim 15^\circ$) structure, Cluster 6, in P5. Clusters constructed using the repeating events analysis are consistent with Clusters 1, 5 and 7 identified by the GMM method. We also highlight two potential structures in P4 and P5 represented by green dots, which have been identified as clusters in certain clustering runs, but not as stable as Cluster 1 to 7.

Clusters constructed using the repeating events analysis are consistent with Clusters 1, 5 and 7 identified by the GMM method. The good agreement in cluster identification between these two independent methods confirms the robustness of our strategy and the identification of these vertically dipping structures. 5 out of 7 focal mechanism solutions demonstrate right-lateral strike-slip faulting (Figure 2). These highly consistent faulting solutions

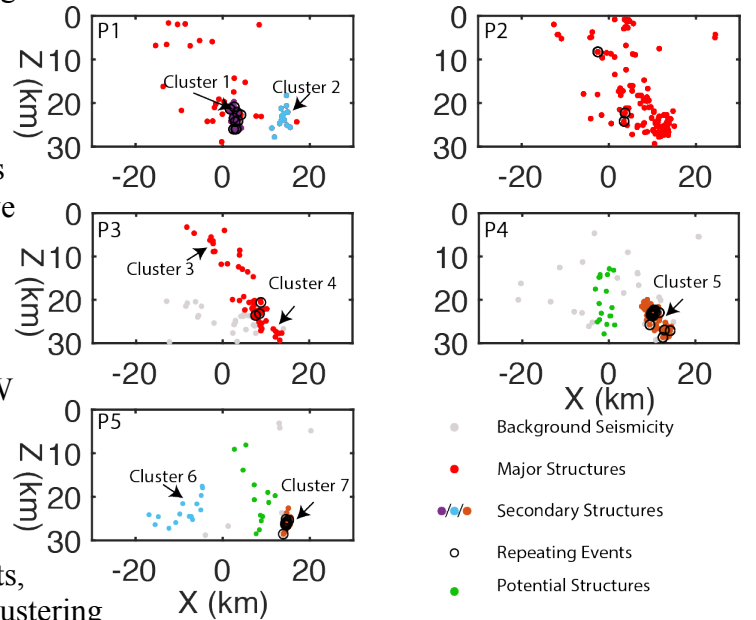


Figure 4. Final results from clustering analysis. Red dots represent seismic clusters determined by GMM method. Grey dots represent background seismicity, i.e. events not constituting a seismic cluster. Black open circles represent repeating event clusters. Yellow dots represent secondary structures.

suggest the general deformation below the LRF is right-lateral, or, at least, the secondary structures delineated by REs tend to slip in the sense of right-lateral mode.

5. Discussions

5.1 Implications on the Leech River Fault Zone

The results drive us to define a potential geometry of a seismogenic structure that varies along strike. We suggest the LRF seismogenic structure consists of one strand in the west (profiles P1-P3) and two branches in the east (P4-P5). Between Leechtown and Victoria (P1-P3) the broadly NE-dipping Leech River fault zone has a finite thickness of 8 to 10 km and dips NNE at $\sim 60^\circ$. This structure splays between P4 and P5 into two branches, with one branch continuing to dip toward NNE and potentially linked to the Devil's Mountain Fault (DMF) and another branch dipping toward the SW potentially linked to the Southern Whidbey Island Fault (SWIF) (Figure 5).

We make this conclusion based on the following two sets of observations of the relocated seismicity and field geology. First, seismicity in profiles P1 and P2 delineates a NNE dipping structure with two vertical secondary structures identified as Clusters 1 and 2 in P1 (Figure 4). For profile P3, the two stable clusters 3 and 4 are considered to form a single $\sim 60^\circ$ NNE dipping structure. The seismicity pattern becomes much more complicated in P4 and P5, as the L/C values decrease to 0.6/0.3 and 0.6/0.01, respectively. These results indicate it is not possible to determine a single structure on the eastern extent of our study area. Second, previous studies show a system of active faults near the LRF extending across the Juan de Fuca strait into an adjacent fault network in NW Washington [Johnson et al., 2001; Barrie and Greene, 2015]. For example, shallow seismic reflection and sediment core data indicate eastern LRF merges along the strike with the western extent of the DMF (which has a 45° to 75° N dip as observed in the upper 2km) and the SWIF (a wide fault zone consist of both northeast-dipping and southwest-dipping faults) across the eastern Juan de Fuca Strait [Wagner and Tomson, 1987; Johnson et al., 2001]. The northern seismic structures identified in this study projects to the western extensions of the DMF (Cluster 5, Cluster 7 and the potential structure in P5). The DMF branch has a NNE dip angle of $\sim 60^\circ$, similar to what is observed between P1 and P3. The potential structures in P4 and Cluster 6 project toward the SWIF. The dip angle of Cluster 6 may suggest that the SWIF branch has a less steep dipping angle at depth. The branching angle between DMF and SWIF fault traces at the surface is $\sim 17^\circ$, consistent with splay angle statistics of natural faults [Ando et al., 2009].

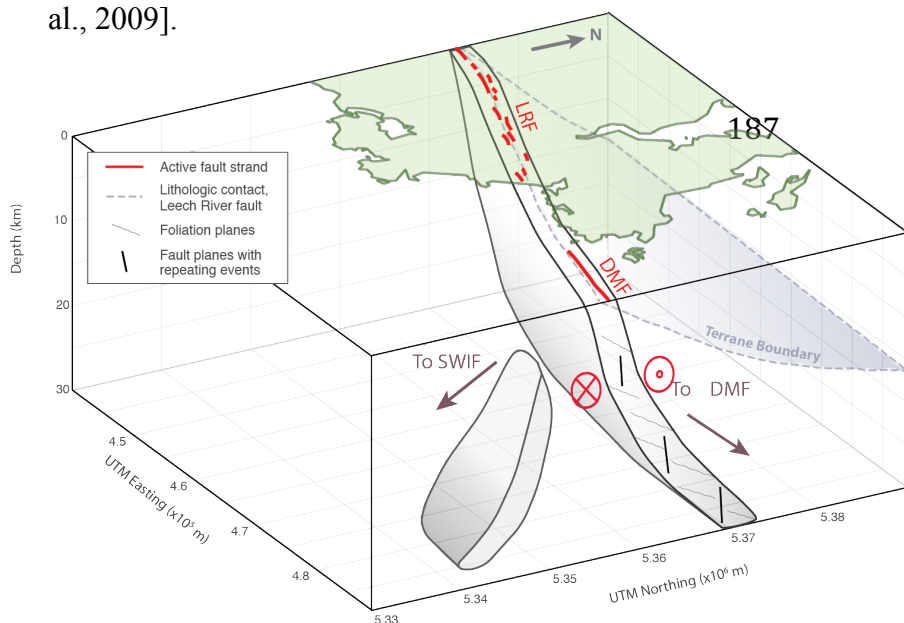


Figure 5. Proposed structural interpretation of the seismicity below the Leech River Fault, showing a broad, steeply-dipping fault zone that bifurcates eastward into two strands that projects into the Devils Mountain Fault (DMF) and Southern Whidbey Island Fault (SWIF). We interpret the relocated seismicity to fall within a broad deformation zone that contains a network of sub vertical fractures that overprints a northeast-dipping structural fabric, and which does not re-occupy the lithologic terrane boundary contact between the Crescent and Pacific Rim terranes.

5.2 Secondary Structures

Based on the GMM and RE methods, we are able to quantitatively and objectively identify 7 vertical structures within the broad Leech River Fault Zone. We interpret these vertical structures as secondary structures developed within the broad LRFZ. Focal mechanisms solutions of some repeating earthquakes suggest the fault zone in general is accommodating right-lateral strike-slip at depth. These secondary structures contribute to define a fracture network as well. First, the near-vertical dip of small structures is consistent with Andersonian predictions of fault geometry for strike-slip, and the general

northward dip of the seismic zone reflects attempted reactivation or inheritance of the north-dipping foliation fabric. The inconsistency between the moderate dipping angle of the proposed major structure and the vertical angle of identified smaller structures suggests these secondary structures may be interpreted as younger, near-vertical fractures imprinting the pre-existing north-dipping foliation fabric. Therefore, our preferred hypothetical model is a deformation zone with a steeply dipping fracture network overprinting a moderately dipping foliation/bedding fabric (Figure 5).

6. Conclusion

Our results thus provide the first evidence to describe crustal seismogenic structures on the southern Vancouver Island using relocated microseismicity. Using HypoDD program, we relocated 1126 out of 1253 CNSN cataloged earthquakes between 1985 and 2015 beneath the southern Vancouver Island, with a focus on events in the upper 30 km in the forearc crust near Leech River Fault zone. We further applied independent clustering techniques to identify seismically active structures of both broad and fine scales and their variation along the LRF. Our results suggest the LRFZ can be interpreted as a NNE dipping deformation zone with two splay structures off shore, which are possibly connected to the Devil's Mountain Fault to the north and the Southern Whidbey Island Fault (SWIF) to the south, respectively. With the observations of secondary structures, defined as vertically dipping fractures accommodating right-lateral slip in depth, we propose the LRFZ is a deformation zone with a steeply dipping fracture network overprinting a moderately dipping foliation/bedding fabric.

References

- Ando R., B. R. Shaw, and C. H. Scholz (2009), Quantifying natural fault geometry: Statistics of splay fault angles, *Bull. Seism. Soc. Am.*, **99**, No.1 pp. 398-395, doi: 10.1785/012008094
- Balfour, N.J., J.F. Cassidy, S.E. Dosso and S. Mazzotti (2011), Mapping crustal stress and strain in southwest British Columbia, *J. Geophys. Res.*, **116**, B03314, doi: 10.1029/2010JB008003.
- Barrie, J. V. and H. G. Greene (2015), Active faulting in the northern Juan de Fuca Strait implications for Victoria, British Columbia, *Geo. Surv. Can.*, Current Research 2015-6, 10 p. doi: 10.4095/296564.
- Cassidy, J. F., G. C., Rogers, and F. Waldhauser (2000), Characterization of active faulting beneath the strait of Georgia, British Columbia, *Bull. Seism. Soc. Am.* **90**, 5, pp. 1188-1199
- Clowes, R. M., M. T. Brandon, A. G. Green, C. J. Yorath, A. S. Brown, E. R. Kanasweich and C. Spencer (1987), LITHOPROBE-southern Vancouver Island: Cenozoic subduction complex imaged by deep seismic reflections, *Can. J. Earth Sci.* VOL. 24
- Gardonio, B., D. Marsan, O. Lengline, B. Enescu, M. Bouchon, and J. Got (2015), Changes in seismicity and stress loading on subduction faults in the Kanto region, Japan, 2011-2014, *J. Geophys. Res. Solid Earth*, **120**, doi:10.1002/2014JB011798
- Hardebeck, J. L. and P. M. Shearer (2003), Using S/P Amplitude Ratios to Constrain the Focal Mechanism of Small Earthquakes, *Bull. Seism. Soc. Am.*, **93**, 2434-2444.
- Johnson, S.Y., S.V. Dadisman, D.C. Mosher, R.J. Blakely and J. R. Childs (2001), Active tectonics of the Devils Mountain Fault and related structures, Northern Puget Lowland and eastern Strait of Juan de Fuca region, Pacific Northwest, U.S. Geological Survey Professions Paper, 164
- Kovacs, P. and R. Sweeting (2004), Earthquake hazard zones: The relative risk of damage to Canadian buildings, The Institute for Catastrophic Loss Reduction Research Paper Series No.39
- Morell, K. D., C. Regalla, L. J. Leonard, C. Amos and V. Levson (2017), Quaternary rupture of a crustal fault beneath Victoria, British Columbia, Canada, *GSA Today*, v.27, doi: 10.1130/GSATG291A.1
- Mosher, D. C., J. F. Cassidy, C. Lowe, Y. Mi, R.D. Hyndman, G.C. Rogers and M. Fisher (2000), Neotectonics in the Strait of Georgia: first tentative correlation of seismicity with shallow geological structure in southwestern British Columbia: Current Research, **A22**
- MacLeod, N. S., D. L. Tiffin, P. D. Snively and R. G. Currie (1977), Geologic interpretation of magnetic and gravity anomalies in the Strait of Juan de Fuca, U.S. - Canada, *Can. J. Earth Sci.*, **14**, 223-238. doi: 10.1139/e77-024.
- McLachlan, G. and D. Peel (2000), Finite Mixture Models, NJ: John Wiley & Sons, Inc.
- Nadeau R.M., W. Foxwall and T. V. McEvilly (1995), Clustering and periodic recurrence of microearthquakes on the San Andres Fault at Parkfield, California, *Science*, **267**, 5197; ProQuest pg.503
- Rogers, G. C. (1994), Earthquakes in Vancouver area, In Geology and Geological Hazards of the Vancouver Region, Southwestern British Columbia. Edited by J.W.H. Monger. *Geological Survey Can. Bull.*, **481**:221-229
- Waldhauser, F., and W. Ellsworth (2000). A double-difference earthquake location algorithm: Method and application to the northern Hayward fault California, *Bull. Seismol. Soc. Am.* **90**, 1353-1368.
- Wagner, H. C., and J. H., Tomson (1987), Offshore geology of the strait of Juan de Fuca, state of Washington and British Columbia: Washington Division of Geology and Earth Resources Open-File Report 87-1